

THE INFLUENCE OF OXYGEN-CONTAINING FUNCTIONAL GROUPS ON THE SURFACE BEHAVIOR AND ROUGHNESS CHARACTERISTICS OF GRAPHENE OXIDE

AHMAD ALLAHBAKHSH

Department of Polymer Engineering

Islamic Azad University, Shiraz Branch, Shiraz, Iran

ahmad.allahbakhsh@gmail.com

FARHAD SHARIF

Department of Polymer Engineering

Amirkabir University of Technology, Tehran, Iran

sharif@aut.ac.ir

SAEDEDEH MAZINANI

Amirkabir Nanotechnology Research Institute (ANTRI)

Amirkabir University of Technology, Tehran, Iran

s.mazinani@aut.ac.ir

Received 21 December 2012

Accepted 11 April 2013

Published 14 May 2013

The effects of oxygen-containing functional groups on the surface roughness of graphene oxide are thoroughly studied using three-dimensional atomic force microscopy images, ball-and-stick model and wire-frame view results. Moreover, X-ray diffraction method and Fourier transform infrared spectroscopy are employed for characterizing the structural and chemical behavior of graphene oxide, respectively. Graphene oxide sheets show a clear concavity on one side when the aggregation of functional groups increased on the other side. This behavior could be the main reason for the surface fluctuation of graphene oxide sheets that is observed in microscopic images. In addition, the individual graphene oxide sheet presents greater values of mean roughness compared to multilayered sheets.

Keywords: Atomic force microscopy; graphene oxide; nanoparticles; oxidation; roughness; surface characterization.

1. Introduction

Graphene is a two-dimensional (2D) structure of sp^2 -bonded carbon atoms which are densely packed in a honeycomb lattice.¹ This individual structure results in high values of modulus, thermal and

electrical conductivity that make graphene promising for many applications.^{2–5} The chemical functionalization of graphene assists the dispersion of graphene in polymer matrix and stabilizes the graphene to prevent agglomeration.⁶ Among the

different reported applications of graphene, the use of graphene as electronically and thermally conductive nanofiller in manufacturing nanocomposites is considered as the most popular application of graphene.^{7–9} However, to achieve enhanced electrical and thermal properties, high degree of exfoliation and dispersion of graphene in polymer matrices is essential.¹⁰ The chemical functionalization of graphene is a reliable way to assist the dispersion of graphene in matrix and stabilizing graphene to prevent agglomeration.⁶

Graphene oxide (GO) is generally prepared through the oxidation of graphite using potent oxidizers followed by the exfoliation of graphite oxide through thermal treatment or ultrasonic processes.^{11–13} The presence of oxygen-containing functional groups such as hydroxyl, carboxyl, carbonyl and epoxide results in a reported increase in the *d*-spacing of GO. Besides, the presence of oxygen-containing functional groups leads to the hybridization of oxidized carbon atoms from planar sp^2 to tetrahedral sp^3 .¹¹ GO is strongly hydrophilic and because of the existence of functional groups attached on the basal or edge of sheets can easily disperse in matrixes. In addition, the presence of oxygen-containing functional groups on the surface of GO leads to a highly fluctuated surface which assists the combination of GO and matrixes.

Nanoroughness is an important factor in nanostructures and nanodevices because it does not scale down with the dimensions of the devices.⁴ Nanoroughness always falls into three aspects including: edge roughness, width roughness and sidewall roughness. Each of these important factors is usually depended to the pattern of processing and deposition of nanoparticle. The practical importance of these factors is in the properties of nanodevices such as the electrical characteristics of transistors, the capacitance of thin insulating films, the light scattering in optoelectronic devices, the absorption of proteins on surfaces, the wettability of the surfaces and many other applications.^{5,9,14,15} As a result, the investigation of nanoroughness and the effects of oxidation and the location of functional groups on this value is a key factor to predict the properties and mix-behavior of GO in different applications.

There are just limited works regarding the surface of the single GO sheet and the effects of oxidation on the atomistic behavior of GO by Schniepp.¹⁶ In this paper, the effects of oxygen-containing functional groups on the surface roughness of GO were fully

examined using atomic force microscopy (AFM) three-dimensional (3D) images as well as ball-and-stick model and wire-frame views. In addition, the influence of different functional groups and the location of these groups on the surface nanoroughness of GO was investigated.

2. Experimental Methods

2.1. Chemicals and materials

Graphite powder was purchased from LECO Co. and potassium permanganate ($KMnO_4$), sulfuric acid (H_2SO_4) and all other reagents and solvents were provided from Merck Chemicals Co.

2.2. Preparation of GO

Natural graphite powder was used for preparing GO by a modification in Hummers and Offeman's method¹⁷ About 1 g of graphite powder was put into a round bottom flask. Thereafter, 100 mL of sulfuric acid (98%) was added into the flask. Afterward, the mixture was stirred and gradually 6 g of $KMnO_4$ was added to the mixture. Once more the mixture was stirred by a magnetic stirrer at room temperature for 2 h. The mixture was subsequently allowed to react for 4 h at 35°C. Then, 300 mL of distilled water was added to the reaction mixture. Followed by 15 min, the reaction was terminated by adding 50 mL of H_2O_2 aqueous solution (25 mL, 30%), resulting in a yellow-brown mixture. Finally, the mixture was centrifuged and washed out for five times with a 10% HCl solution and was repeatedly washed out with water till the neutral pH of the filtrate was reached.

Graphite oxide was dispersed in water (5 mg/mL) and sonicated (20 kHz, 1000 W, 80% power) for 20 min. In order to remove un-exfoliated GO particles, the mixture was centrifuged for 10 min at 5000 rpm to obtain the GO suspension. GO suspension was gradually sprayed out on a glass surface kept at 110°C and then was separated layer by layer from the surface to achieve GO nanosheets powder. The procedure of GO powder preparation was naive and efficient and led to multilayer GO powders formation.

2.3. Characterization methods

AFM were provided using a Dualscope DS 95–200, DME. Samples for AFM were developed on a freshly cleaved mica surface. Chemical characteristics of GO

were characterized by Nicolet IR100 FT-IR spectrometer. X-ray diffraction (XRD) patterns were presented on an Inel Equinox 3000 diffractometer (CuK_{α} ($\lambda = 1.54056 \text{ \AA}$) at 40 kV and 30 mA). Hielscher UIP1000hd homogenizer (20 kHz, 1000 W) was used for the ultrasonic process. Roughness parameters, force field analyses and wire-frame model 3D views were computed using a Femtoscan image processing software (version 2.3.94), Avogadro molecule editor software (version 1.0.3) and Femtoscan image processing software, respectively.

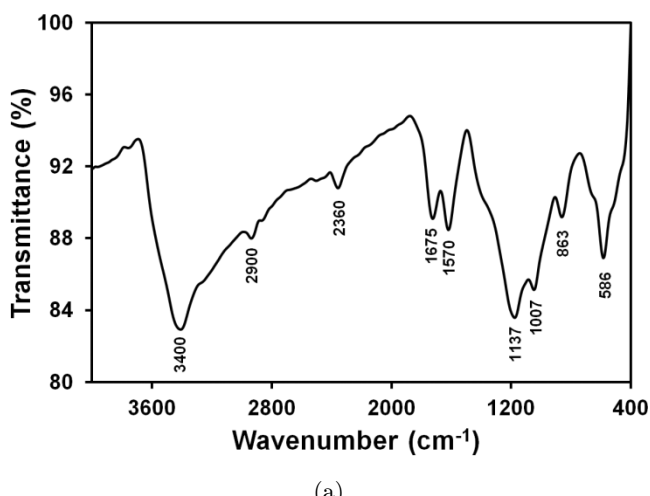
3. Results and Discussion

FTIR and XRD techniques were employed to characterize the chemical and structural behaviors of GO as shown in Fig. 1. The FTIR spectrum of GO [see Fig. 1(a)] showed two peaks around 586 cm^{-1} and 863 cm^{-1} mainly corresponding to C–H deformation vibration. The absorption peaks at 1007 cm^{-1} and 1137 cm^{-1} were contributed to C–O–C bond stretching in the structure of epoxide group.¹⁸ Moreover, the peak around 1570 cm^{-1} and 3400 cm^{-1} were corresponding to C–OH stretching vibrations in hydroxyl groups and C=C stretching vibrations, respectively.^{18,19} Furthermore, vibration peaks at 1675 cm^{-1} and 2900 cm^{-1} were corresponding to C=O and C–H stretching vibrations, respectively.^{20,21} In addition, a peak that appeared around 2360 cm^{-1} was contributed to C–H deformation vibration. Moreover, the XRD pattern of the pristine graphite [see Fig. 1(b)] contained a sharp reflection peak at $2\theta = 26^\circ$ which originated from the interlayer

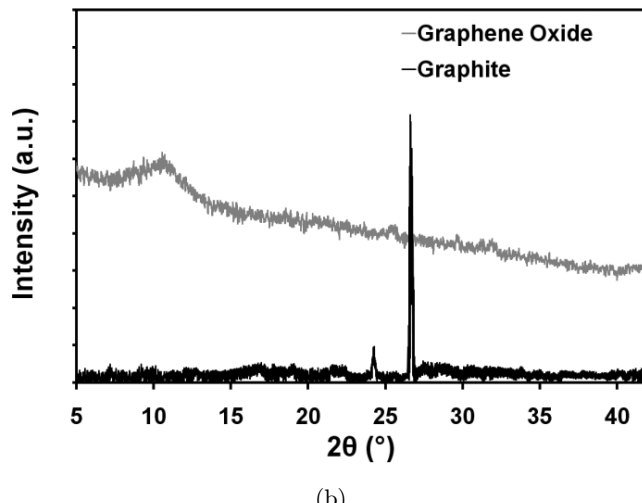
spacing of $d = 0.34 \text{ nm}$. Upon oxidation, adjacent layers were $\sim 0.8 \text{ nm}$ apart ($2\theta = 11^\circ$) due to the presence of oxygen-containing functional groups.

AFM was employed to characterize the thickness distribution of GO sheets, as shown in Fig. 2. The thickness of an individual GO sheet was about 1.5 nm and thickness of few-layered GO sheets was in the average range of 1.5–2.5 nm. In addition, Avogadro software was used to study the effects of oxygen-containing functional groups on the surface behavior of GO and the location of these attached groups on the force field behavior of sheets. For this purpose, different amounts of epoxide and hydroxyl groups were located in different locations on the surface of an individual sheet and geometry optimization was applied as shown in Fig. 3. Three different possible placements were applied on the surface of an individual sheet and the possible height distribution of GO sheets was investigated. The effects of epoxide groups on the height distribution of sheets were clearly more than those of hydroxyl groups. This behavior probably leads to more influence of epoxide groups on the surface fluctuation and surface roughness of GO sheets compared to hydroxyl ones.¹⁶

AFM 3D images and 3D ball-and-stick model prediction results were used to investigate the effects of functional groups on the surface profile and roughness behavior of an individual sheet and multilayered GO sheets as shown in Fig. 4. As obtained from AFM 3D views, the GO surface was rough in nanoscopic scale including some wrinkles which can be referred to the existence of oxygen-containing functional groups. The influence of



(a)



(b)

Fig. 1. Characterization of GO: FTIR spectrum of GO (a) and XRD patterns of pristine graphite and GO nanosheets (b).

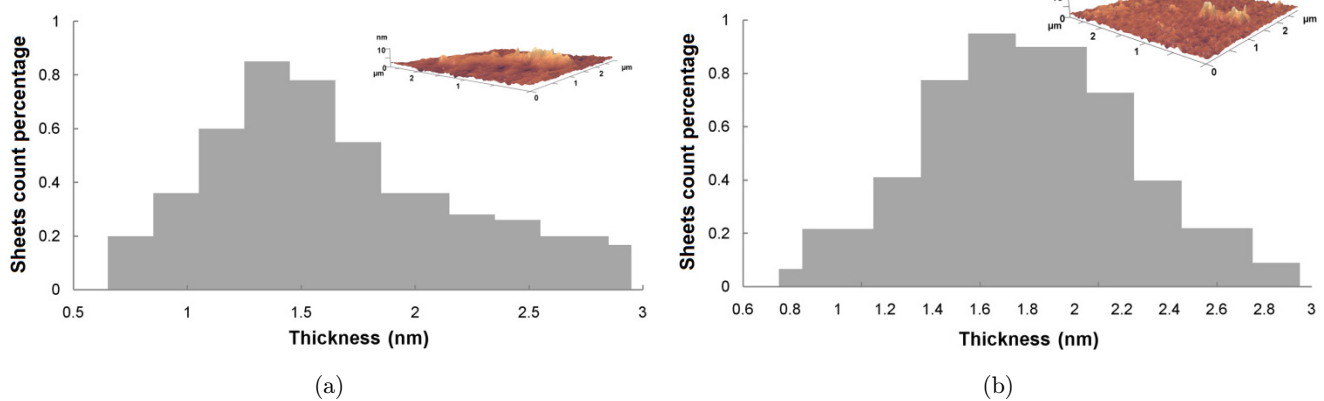


Fig. 2. Thickness histograms of an individual GO sheet (a) and multilayered GO sheets (b).

oxygen-containing functional groups on the surface behavior of GO was predicted using ball-and-stick model of an individual GO sheet. For this, a combination of epoxide and hydroxyl functional groups were placed on a specific area of a graphene single sheet. This area was selected based on the specific area of the sheet with more sheet height in 3D AFM views. However, as the influence of epoxide groups on the height increments were clearly more than that of the hydroxyl [see force field analysis in Figs. 3(a) and 3(b)], the number of epoxide groups

was more than hydroxyl groups in simulation geometry.

Obviously, the sheet height increased noticeably in simulated geometry with more aggregation of the functional groups on a specific area of GO sheet. This behavior was observed in ball-and-stick simulation of both individual and multi-layered GO sheets (see Fig. 4). The height of GO sheets increases

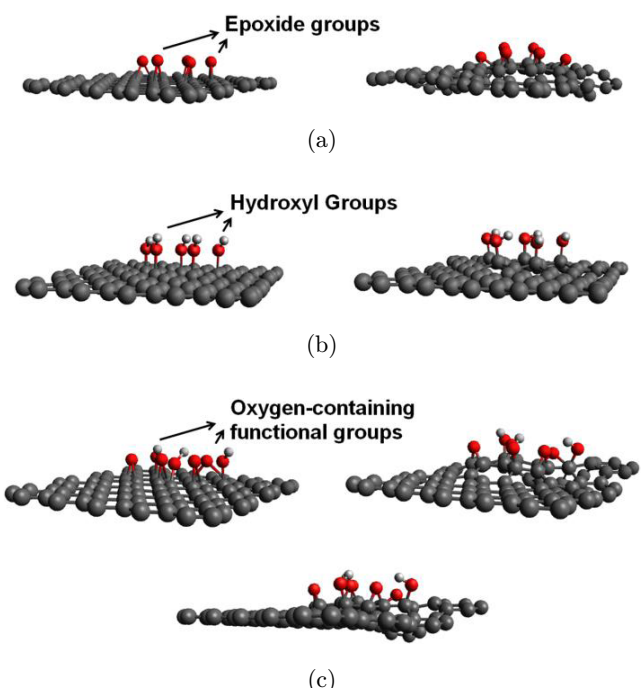


Fig. 3. Force field analysis of an individual GO sheet with the placement of epoxide (a) hydroxyl (b) and epoxide-hydroxyl (c) functional groups.

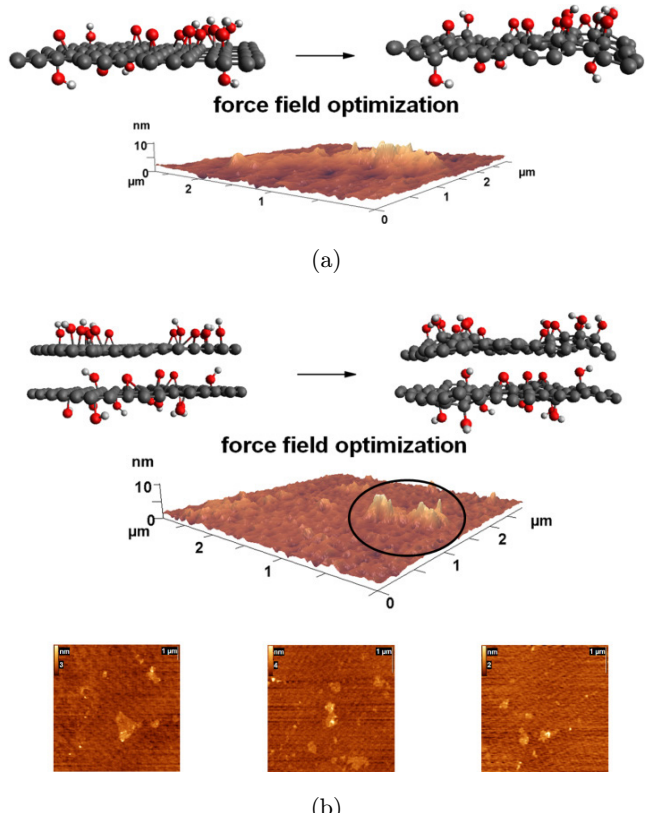


Fig. 4. Force field analysis of an individual GO sheet (a) and GO sheets in bulk (b) in the presence of functional groups using ball-and-stick prediction model and AFM 3D and 2D views.

through oxidation process due to the shrinkage of the GO sheets hexagonal rings. This shrinkage is because of an increase in the length of the C–C bonds in the structural hexagonal rings of the sheets in the presence of oxygen-containing functional groups.²²

GO sheets showed a clear concavity on one side when the aggregation of functional groups increased on the other side. This behavior can be regarded as the main reason for the surface fluctuation of GO sheets observed in AFM 3D images.¹⁶ The exact location of attached functional groups on the surface of GO in suspension form is unpredictable. However, the location of functional groups aggregations on the surface of GO could be predicted on the peaks of 3D AFM views according to the results of ball-and-stick model. In addition, the height of GO sheets in bulk mode increased to 11.69 ± 0.95 nm [calculated for 10 GO nanosheets through three cross-sections in Fig. 4(b)]. This behavior is probably related to the interactions between the surfaces of adjacent layers.

The wire-frame model and AFM 3D views of individual and multilayered sheets were employed for further investigation of the surface roughness of GO sheets, as shown in Fig. 5. The wire-frame 3D views clearly showed wrinkled and fluctuated surface of GO sheets. This high degree of fluctuation on the surface of GO was contributed to the presence of these wrinkles which were attributed to the aggregations of functional groups. Furthermore, the wire-frame 3D view of GO sheets in bulk mode represented a clear view of surface behavior of multilayered GO sheets which contained more wrinkles compared to an individual sheet [see Fig. 5(e)].

Surface roughness of 2D materials such as GO sheets is very important for many fundamental problems such as tightness of contact joints as well as heat and electric conduction.²³ The tightness of contact joints of GO sheets is an important factor in the incorporation of this nanofiller in the preparation of nanocomposites. In addition, one of the most interested applications of the graphene-based materials is in electrical nanodevices. Therefore, the GO surface roughness is an important factor for the fabrication of high-performance nanodevices and composites.

The main roughness parameters of AFM images were used to study the surface roughness of individual and multilayered GO sheets, as summarized in Table 1. The values of mean roughness (R_a) and

root mean square roughness (R_q) represent the arithmetic average of the surface height values and the standard deviation of feature height of GO sheets, respectively. Moreover, the peak–peak height (R_z) parameter represents the arithmetic mean value of the highest peaks and the lowest valley depth within a cross-section and is an evidence for the degree of surface fluctuation. In addition, the value of surface skewness (R_{sk}) describes the asymmetry of the height distribution histogram of sheets. Furthermore, the surface kurtosis (R_{ku}) describes the peakedness of the surface topography.²³ The average values of parameters extracted from eight different cross-sections were used to calculate the roughness parameters (see Fig. 6 and Table 1).

The values of R_a and R_q for an individual GO sheet were about 0.2 nm and 0.3 nm greater than the same parameters for multilayered sheets in bulk, respectively. This behavior could be referred to two possible reasons: the degree of exfoliation and oxidation of GO sheets. The oxidation process of an individual GO sheet resulted in a high degree of surface fluctuation due to the thin thickness of GO sheet. On the other hand, the intercalation of oxidizers within GO sheets probably decreased because of the molecular diffusion limitations and as a result the oxidation of graphite sheets reduced. This behavior led to a decrease in the distribution of oxygen-containing functional groups on the surface of multilayered GO sheets. Besides, the values of root mean square roughness for GO were reported about 1.2 nm in literatures.²⁴

The greater value of R_z for multilayered sheets explains the greater bend of the sheets because of the aggregation of functional groups and the broader distribution of these groups on the surface of GO sheets. Moreover, the values of R_{sk} and R_{ku} for multilayered GO sheets in bulk were reported about 0.9 and 3 units greater than the same parameters for individual sheets, respectively. The values of R_{sk} beyond 1.0 represent extreme numbers of peaks on the surface of the sheet. Besides, the values of R_{ku} beyond 3.0 indicate narrow height distribution on the surface. Clearly, the aggregation of functional groups on the surface of GO sheets resulted in the extreme amounts of peaks with high intensity on the surface of multilayered sheets. The reported roughness values of GO sheets were in close accordance with the 3D views of wire-frame simulations (see Fig. 5). As depicted, the surface of individual sheets was rougher and the distribution of

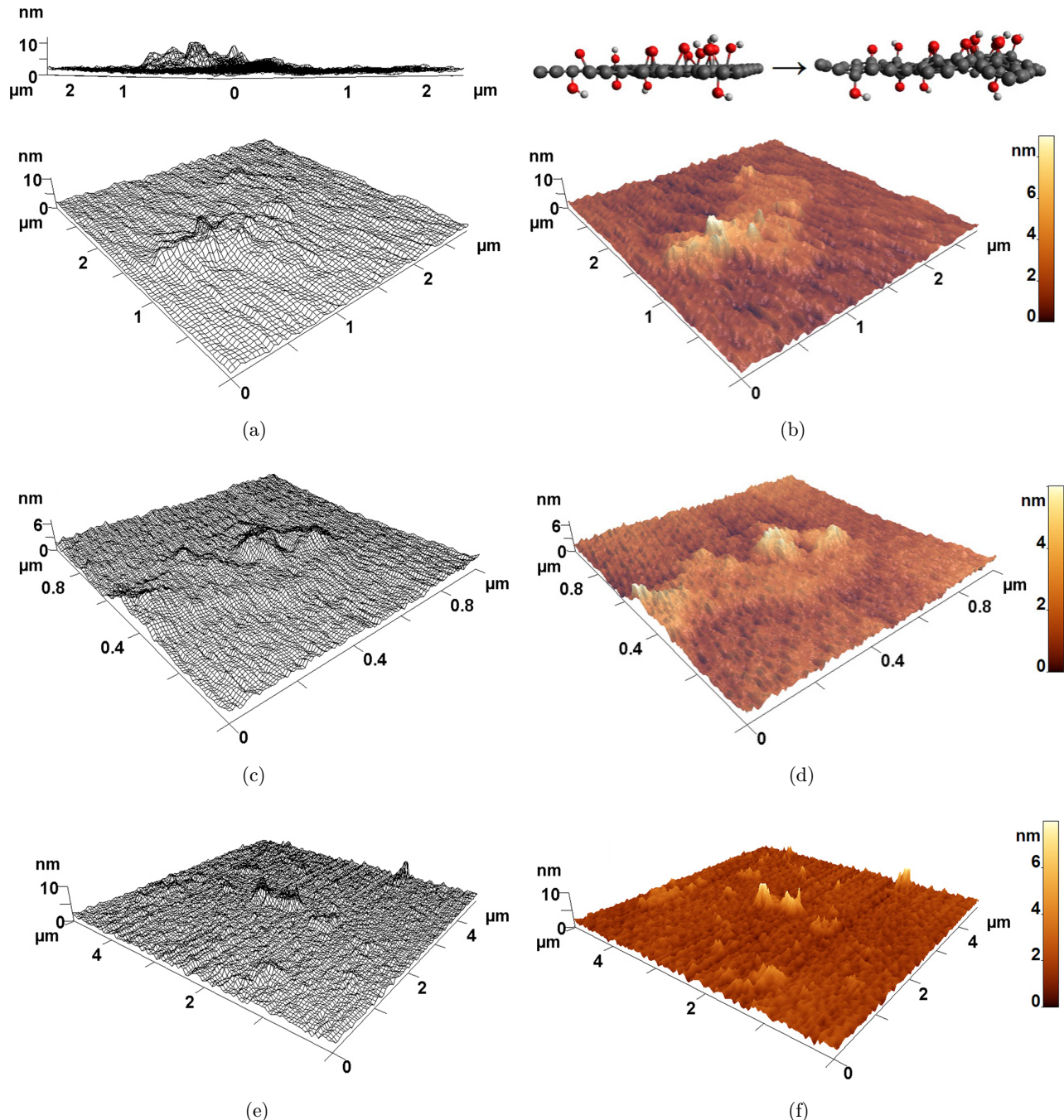


Fig. 5. Wire-frame model 3D views of individual GO sheets (a, c) and multilayered GO sheets (e) as well as related AFM 3D images of individual GO sheets (b, d) and GO sheets in bulk (f).

Table 1. Quantitative roughness parameters of GO.

Roughness parameters	R_a (nm)	R_q (nm)	R_z (nm)	R_{sk}	R_{ku}
Individual sheet	0.792 ± 0.047^a	1.017 ± 0.055	1.072 ± 0.064	0.468 ± 0.946	3.253 ± 0.402
Multi-layered sheets	0.619 ± 0.019	0.729 ± 0.082	1.826 ± 0.094	1.362 ± 0.094	5.899 ± 0.183

^aRoughness parameter \pm standard deviation.

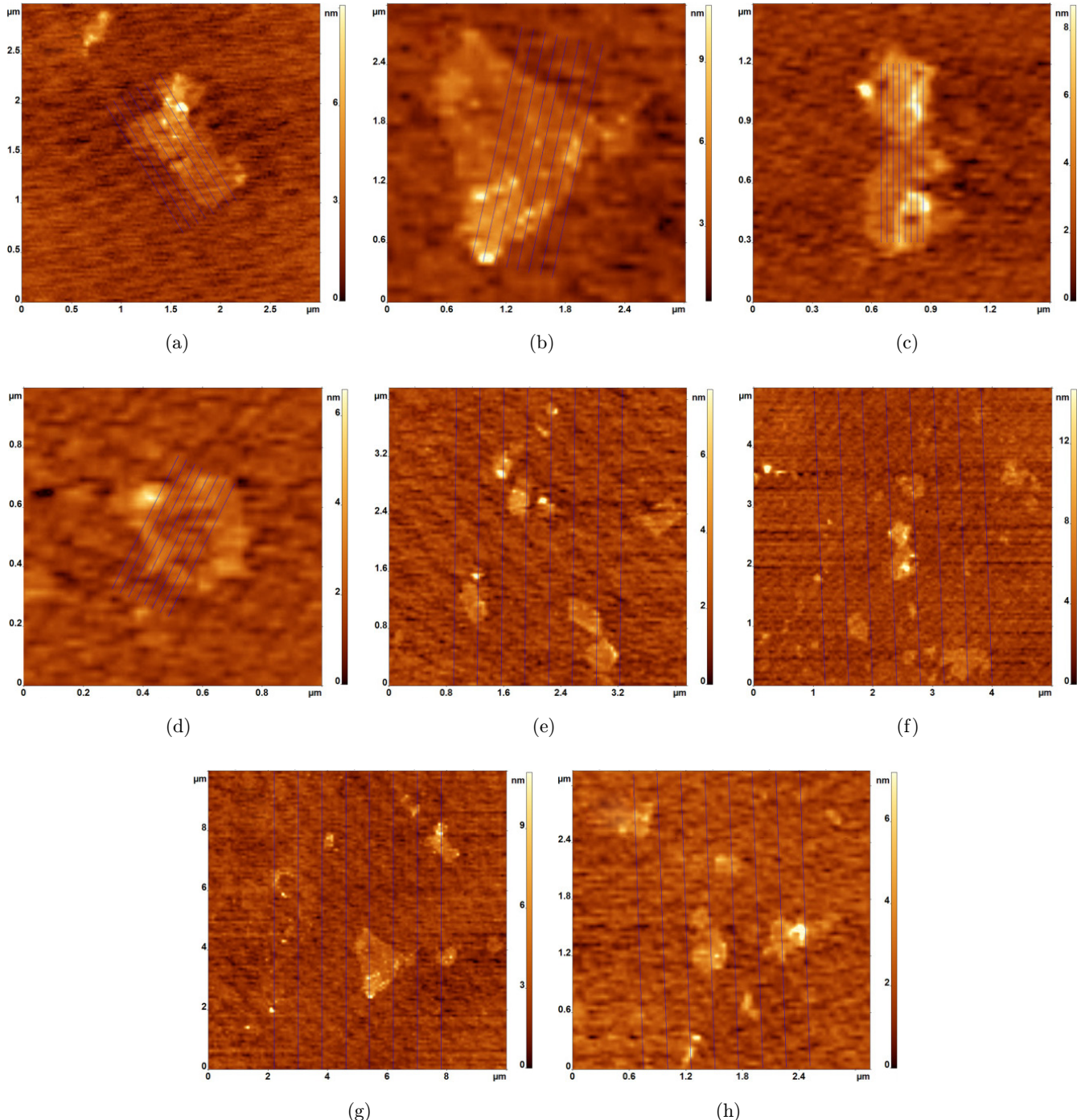


Fig. 6. Cross-sections used in this study for calculating roughness parameters of individual GO sheets (a, b, c and d) and GO sheets in bulk (e, f, g and h).

peaks was broader in comparison with multilayered GO sheets.

4. Conclusions

The surface roughness of synthesized GO was studied using AFM images and 3D simulations. In

addition, the effects of oxygen-containing functional groups on the surface behavior of GO sheets were studied using ball-and-stick model and wire-frame simulations. The high degree of surface fluctuation was observed in AFM 3D images of GO sheets. This behavior was related to the clear concavity of GO sheets which itself was related to an increase in the

aggregation of oxygen-containing functional groups on the other side. In addition, the R_a and R_q values of individual GO sheet were greater than the same parameters for multilayered GO sheets which explained rougher surface of individual sheets. Furthermore, the surface of multilayered GO sheets included extreme amounts of peaks with high intensity because of the large amount of aggregated functional groups.

Acknowledgments

I would like to thank Milad Sheydaeи for his valuable technical help and comments.

References

1. A. K. Geim and K. S. Novoselov, *Nat. Mater.* **6**, 183 (2007).
2. F. Scarpa, S. Adhikari and A. Srikantha Phani, *Nanotechnology* **20**, 065709 (2009).
3. N. Yang, J. Zhai, M. Wan *et al.*, *Synth. Met.* **160**, 1617 (2010).
4. Y. Ren, C. Zhu, W. Cai *et al.*, *Nano* **07**, 1150001 (2012).
5. L. Y. Huang, Q. Han and Y. J. Liang, *Nano* **07**, 1250033 (2012).
6. T. Wei, G. Luo, Z. Fan *et al.*, *Carbon* **47**, 2296 (2009).
7. D. R. Dreyer, S. Park, C. W. Bielawski *et al.*, *Chem. Soc. Rev.* **39**, 228 (2010).
8. J. Wang, Y. Wang, D. He *et al.*, *Synth. Met.* **160**, 2494 (2010).
9. A. L. I. Koochi, A. Kazemi and M. Abadyan, *Nano* **06**, 419 (2011).
10. J. Wang, X. Wang, C. Xu *et al.*, *Polym. Int.* **60**, 816 (2011).
11. M. J. McAllister, J.-L. Li, D. H. Adamson *et al.*, *Chem. Mater.* **19**, 4396 (2007).
12. H. C. Schniepp, J.-L. Li, M. J. McAllister *et al.*, *J. Phys. Chem. B* **110**, 8535 (2006).
13. S. Wang, M. Tamraparni, J. Qiu *et al.*, *Macromolecules* **42**, 5251 (2009).
14. A. Ranella, M. Barberoglou, S. Bakogianni *et al.*, *Acta Biomater.* **6**, 2711 (2010).
15. W. Zhou, X. Zhong, X. Wu *et al.*, *Surf. Coat. Technol.* **200**, 6155 (2006).
16. H. C. Schniepp, J.-L. Li, M. J. McAllister, *et al.*, *J. Phys. Chem. B* **110**, 8535 (2006).
17. W. S. Hummers and R. E. Offeman, *J. Am. Chem. Soc.* **80**, 1339 (1958).
18. Y. Xu, Y. Wang, J. Liang *et al.*, *Nano Res.* **2**, 343 (2009).
19. S. Stankovich, R. D. Piner, S. T. Nguyen *et al.*, *Carbon* **44**, 3342 (2006).
20. Z. Mo, Y. Sun, H. Chen *et al.*, *Polymer* **46**, 12670 (2005).
21. Y. Matsuo, K. Kume, T. Fukutsuka *et al.*, *Carbon* **41**, 2167 (2003).
22. F. Gunes, G. H. Han, H.-J. Shin *et al.*, *Nano* **06**, 409 (2011).
23. E. S. Gadelmawla, M. M. Koura, T. M. A. Maksoud *et al.*, *J. Mater. Process. Technol.* **123**, 133 (2002).
24. H. A. Becerril, J. Mao, Z. Liu *et al.*, *ACS Nano* **2**, 463 (2008).